Syntheses, Crystal Structures, and NLO Properties of New Chiral Inorganic Chromophores for Second-Harmonic Generation

Géraldine Lenoble, Pascal G. Lacroix,* and Jean Claude Daran

Laboratoire de Chimie de Coordination, CNRS, 205 route de Narbonne, 31077 Toulouse Cedex, France

Santo Di Bella

Dipartimento di Scienze Chimiche, Università di Catania, 95125 Catania, Italy

Keitaro Nakatani

PPSM, Ecole Normale Supérieure de Cachan, Avenue du Président Wilson, 94235 Cachan, France

Received April 25, 1997

A new chiral ligand (H_2L) based on the condensation of diaminocyclohexane and 4-(diethylamino)salicylaldehyde is reported along with its nickel(II) and manganese(III) complexes. These compounds all crystallize in noncentrosymmetric space groups. Crystal data are as follows. For the ligand ($C_{28}H_{40}N_4O_2$): monoclinic, *I*2, $a = 15.487(2)$ Å, $b = 8.1988(6)$ Å, $c = 20.958(3)$ Å, $\beta = 95.92(1)°$, $Z = 4$. For the $Ni^{II}L$ complex: monoclinic, $P2_1$, $a = 8.613(2)$ Å, $b = 21.714(4)$ Å, $c = 15.870(4)$ Å, $\beta = 91.02(2)°$, $Z = 4$. For the $Mn^{III}LCl$ complex: orthorhombic, $P2_12_12_1$, $a = 7.233(2)$ Å, $b = 15.159(4)$ Å, $c = 25.591(7)$ Å, $Z = 4$. The manganese derivative exhibits an efficiency 8 times that of urea in second-harmonic generation at 1.9 μm. INDO/SCI−SOS quantum-chemical calculations predict a sizable molecular nonlinear response and an enhancement of the nonlinearity after metal complexation.

Introduction

Second-order nonlinear optical (NLO) properties of molecular materials have attracted a lot of attention especially for their potential application in the newly emerging field of optoelectronics.[1,2] Crucial prerequisites for achieving a large second-order NLO response are that the individual constituents have large molecular responses $\beta(-2\omega;\omega,\omega)$ (step 1) and that they be arranged in an acentric environment to contribute to an observable bulk effect ($\chi^{(2)}$) (step 2).[2c] To date, interest has focused mostly on organic molecules[1,2] and to a far less extent on organometallic compounds.[3−9] Very few studies have been devoted to inorganic molecular systems;[10−15] among them, bis-(salicylaldiminato)-based complexes have appeared to be a promising family of efficient chromophores.[14,15] In a previous paper, we reported donor−acceptor bis(salicylaldiminato)metal-(II) Schiff-base complexes (metal = nickel, copper, zinc) exhibiting the largest molecular responses in this family of chromophores (**I**).[15] However, all these systems crystallize in

(1) (a) Lindsay, G. A.; Singer, K. D. *Polymers for Second-Order Nonlinear Optics*; ACS Symposium Series 601, American Chemical Society: Washington, DC, 1995. (b) Zyss, J. *Molecular Nonlinear Optics*; Academic Press: New York, 1994. (c) Prasad, N. P.; Williams, D. J. *Introduction to Nonlinear Optical Effects in Molecules and Polymers*; Wiley: New York, 1991. (d) Chemla, D. S.; Zyss, J. *Nonlinear Optical Properties of Organic Molecules and Crystals*; Academic Press: Orlando, FL, 1987; Vols 1 and 2.

(2) (a) Benning, R. G. *J. Mater. Chem.* **1995**, *5*, 365. (b) Dalton, L. R.; Harper, A. W.; Ghosn, R.; Steir, W. H.; Ziari, M.; Fetterman, H.; Shi, Y.; Mustacich, R. V.; Jen, A. K.-Y.; Shea, K. J. *Chem. Mater.* **1995**, *7*, 1060. (c) Williams, D. J. *Angew. Chem., Int. Ed. Engl.* **1984**, *23*, 690.

(3) For recent reviews on NLO organometallics, see: (a) Long, N. J. *Angew. Chem., Int. Ed. Engl.* **1995**, *34*, 21. (b) Marder, S. R. In *Inorganic Materials*; Bruce, D. W., O'Hare, D., Eds.; John Wiley & Sons: New York, 1992; pp 115−164.

(4) (a) Whittall, I. R.; Humphrey, M. G.; Houbrechts, S.; Persoons, A.; Hockless, D. C. R. *Organometallics* **1996**, *15*, 5738. (b) Whittall, I. R.; Humphrey, M. G.; Hockless, D. C. R.; Skelton, B. W.; White, A. H. *Organometallics* **1995**, *14*, 3970.

(5) (a) Kanis, D. R.; Lacroix, P. G.; Ratner, M. A.; Marks, T. J. *J. Am. Chem. Soc.* **1994**, *116*, 10089. (b) Kanis, D. R.; Ratner, M. A.; Marks, T. J. *J. Am. Chem. Soc.* **1992**, *114*, 10339.

(6) (a) Coe, B. J.; Hamor, T. A.; Jones, C. J.; McCleverty, J. A.; Bloor, D.; Cross, G. H.; Axon, T. L. *J. Chem. Soc., Dalton Trans.* **1995**, 673. (b) Coe, B. J.; Foulon, J. D.; Hamor, T. A.; Jones, C. J.; McCleverty, J. A.; Bloor, D.; Cross, G. H.; Axon, T. L. *J. Chem. Soc., Dalton Trans.* **1994**, 3427. (c) Houlton, A.; Jasim, N.; Roberts, R. M. G.; Silver, J.; Cunningham, D.; Mcardle, P.; Higgins, T. *J. Chem. Soc., Dalton Trans.* **1992**, 2235.

(7) Loucif-Saïbi, R.; Delaire, J. A.; Bonazzola, L.; Doisneau, G.; Balavoine, G.; Fillebeen-Khan, T.; Ledoux, I.; Puccetti, G. *Chem. Phys.* **1992**, *167*, 369.

(8) (a) Wright, M. E.; Toplikar, E. G.; Lackritz, H. S.; Kerney, J. T. *Macromolecules* **1994**, *27*, 3016. (b) Wright, M. E.; Sigman, M. S. *Macromolecules* **1992**, *25*, 5(22), 6055.

(9) Cheng, L. T.; Tam, W.; Meredith, G. R.; Marder, S. R. *Mol. Cryst. Liq. Cryst.* **1990**, *189*, 137.

(10) Bougault, M.; Mountassir, C.; Le Bozec, H.; Ledoux, I.; Pucetti, G.; Zyss J. *J. Chem. Soc., Chem. Commun.* **1993**, 1623.

(11) Zyss, J.; Dhenaut, C.; Chauvan, T.; Ledoux, I. *Chem. Phys. Lett.* **1993**, *206*, 409.

(12) Thami, T.; Bassoul, P.; Petit, M. A.; Simon, J.; Fort, A.; Barzoukas, M.; Villaeys, A. *J. Am. Chem. Soc.* , **1992**, *114*, 915.

(13) Cummings, S. D.; Cheng, L. T.; Eisenberg, R. *Chem. Mater.* **1997**, 9, 440.

(14) (a) Di Bella, S.; Fragalà, I.; Ledoux, I.; Marks, T. J. *J. Am. Chem. Soc.* **1995**, *117*, 9481. (b) Di Bella, S.; Fragalà, I.; Ledoux, I.; Diaz-Garcia, M. A.; Lacroix, P. G.; Marks, T. J. *Chem. Mater.* **1994**, *6*, 881. (c) Di Bella, S.; Fragalà, I.; Ledoux, I.; Diaz-Garcia, M. A.; Marks, T. J. *J. Am. Chem. Soc.* **1997**, *119*, 9550.

(15) Lacroix, P. G.; Di Bella, S.; Ledoux, I. *Chem. Mater.* **1996**, *8*, 541.

S0020-1669(97)00481-3 CCC: $15.00
Published on Web 04/14/1998

a centrosymmetric or pseudocentrosymmetric environment; thus a vanishing bulk NLO response is achieved.

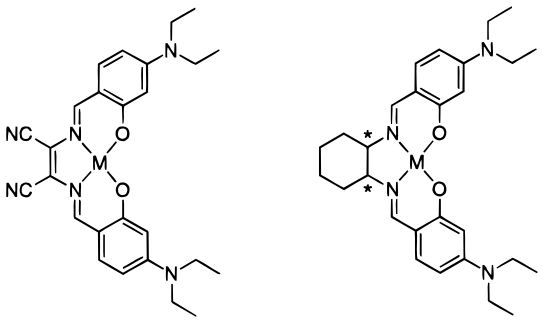

I **II**

The second step of our investigations is reported here as an attempt to engineer these promising chromophores into acentric bulk arrangements of chiral molecular structures. Our strategy was motivated by the careful theoretical examination of molecule **I**. It was pointed out that the "C═N−C" linkage plays an important role as the withdrawing counterpart of the chromophore,[15] whereas the contribution of the nitrile substituent is weak. Thus, molecule **II** was selected in which the "C═N−C" linkage is present, with the addition of two asymmetric carbon atoms to force the crystallization into a noncentrosymmetric space group. The NLO properties of the free ligand H_2L and ML (M = Ni(II), Mn(III)) complexes will be discussed with relation to their crystal structures and their molecular hyperpolarizabilities.

Experimental Section.

Materials and Equipment. (1*R*,2*R*)-(−)-1,2-Diaminocyclohexane (Aldrich) and 4-(diethylamino)salicylaldehyde (Janssen) were used without further purification. Elemental analyses were performed by the Service de Microanalyses du Laboratoire de Chimie de Coordination, Toulouse, France. UV−vis spectra were recorded in various solvents on a Hewlett-Packard 8452A spectrophotometer and ^{1}H NMR spectra on a Bruker AM 250 spectrometer. Mass spectra were acquired on a Nermag R 10-10 instrument. The magnetic susceptibility of the Mn(III) derivative was recorded at room temperature on a Faraday type magnetometer.

Ligand (H_2L) Synthesis. (1*R*,2*R*)-(−)-1,2-Diaminocyclohexane (114 mg, 10^{-3} mol) and 4-(diethylamino)salicylaldehyde (386 mg, 2×10^{-3} mol) were refluxed for 2 days in 100 mL of toluene with a Dean Stark apparatus. An impurity of the yellow monoimine was removed by chromatography on silica, using CH_3OH as an eluent (75% yield). ^{1}H NMR ($CDCl_3$), δ: 1.14 (t, J = 7.1 Hz, 12H, CH_2CH_3), 1.40 (m, 2H, cyclohexyl), 1.63 (m, 2H, cyclohexyl), 1.80−1.95 (m, 4H, cyclohexyl), 3.14 (m, 2H, cyclohexyl), 3.31 (q, J = 7.1 Hz, 8H, CH_2CH_3), 6.02 (dd, J = 5.1 and 2.4 Hz, 2H, aromatic), 6.07 (d, J = 2.4 Hz, 2H, aromatic), 6.88 (d, J = 8.6 Hz, 2H, aromatic), 7.92 (s, 2H, C*H*═N), 13.16 (broad, 2H, O*H*). Mass spectrum (DCI/NH_3), *m*/*z* (% relative intensity): 465 (MH^+, 100), 466 (32), 467 (5). Anal. Calcd (found) for $C_{28}H_{40}N_4O_2$: C, 72.38 (71.29); H, 8.68 (8.39); N, 12.06 (12.25). Single crystals were grown by slow evaporation of a solution of the pure Schiff base in ethanol.

Complex Syntheses. (a) NiL·EtOH. A solution of 114 mg (10^{-3} mol) of (1*R*,2*R*)-(−)-1,2-diaminocyclohexane in 10 mL of absolute ethanol was added to a mixture of $NiCl_2 \cdot 6H_2O$ (238 mg, 10^{-3} mol) and 4-(diethylamino)salicylaldehyde (386 mg, 2×10^{-3} mol) dissolved in 50 mL of hot absolute ethanol, and the resulting red solution was refluxed for a few hours. Large cubic crystals were obtained after cooling and slow evaporation (85% yield). ^{1}H NMR ($CDCl_3$), δ: 1.13 (t, J = 7.1 Hz, 12H, CH_2CH_3), 1.2−1.4 (m, 4H, cyclohexyl), 1.85 (m, 2H, cyclohexyl), 2.37 (m, 2H, cyclohexyl), 2.93 (m, 2H, cyclohexyl), 3.30 (q, J = 7.1 Hz, 8H, CH_2CH_3), 6.00 (dd, J = 8.9 and 2.2 Hz, 2H, aromatic), 6.21 (d, J = 2.0 Hz, 2H, aromatic), 6.86 (d, J = 8.8 Hz, aromatic), 7.10 (s, 2H, C*H*═N). ^{1}H NMT (ethanol), δ: 1.24 (t, 3H, J = 7.0), 3.71 (m, 2H). Anal. Calcd (found) for $C_{28}H_{38}N_4NiO_2 \cdot C_2H_5OH$: C, 63.51 (63.35); H, 7.82 (7.25); N, 9.87 (9.11).

(b) MnLCl. To a solution of 114 mg (10^{-3} mol) of (1*R*,2*R*)-(−)-1,2-diaminocyclohexane and 386 mg (2×10^{-3} mol) of 4-(diethylamino)salicylaldehyde in 40 mL of hot absolute ethanol was added 198 mg (10^{-3} mol) of $MnCl_2 \cdot 4H_2O$. The resulting red solution was refluxed, and 80 mg (2×10^{-3} mol) of NaOH was added, which was followed by slow precipitation of the crude compound. Single crystals were obtained by recrystallization in CH_3CN (30% yield). Anal. Calcd (found) for $C_{28}H_{38}ClMnN_4O_2$: C, 60.81 (60.50); H, 6.93 (6.91); N, 10.13 (10.09).

X-ray Data Collections and Structure Determinations. Single crystals were grown by slow crystallization as described in the above synthetic procedure. For MnLCl, data were collected at room temperature on an Enraf-Nonius CAD4 diffractometer whereas, for H_2L and NiL·EtOH, they were collected at 180 K and room temperature, respectively, on a Stoe IPDS (imaging plate diffraction system) diffractometer. The final unit cell parameters for the Mn(III) derivative were obtained by least-squares refinement of the setting angles of 25 reflections accurately centered on the diffractometer. For the two other compounds, the final unit cell parameters were derived from the least-squares refinement of 5000 selected reflections. Only statistical fluctuations were observed in the intensity monitored over the course of the data collections.

The three structures were solved by direct methods (SIR92)[16] and refined by least-squares procedures on F_{obs}. H atoms were located on difference Fourier maps, but they were introduced in the calculations in idealized positions (d(CH) = 0.96 Å) and their atomic coordinates were recalculated after each cycle. They were given isotropic thermal parameters 20% higher than those of the carbon to which they are attached. Only the H atoms bound to O atoms in the free ligand H_2L were refined with an equivalent isotropic thermal parameter. In NiL·EtOH, the two solvent ethanol molecules present in the crystal cell are disordered with the ethyl groups distributed on two sites related by a pseudo-2-fold axis passing through the O atoms. The absolute configuration for all compounds were examined by refining the Flack's enantiopole parameter **x** defined as $F_o2 = (1 - \mathbf{x})\, F(h)^2 + \mathbf{x}\, F(-h)^2$.[17] The absolute configuration cannot be determined reliably for the free ligand, whereas for both the metal complexes, the **x** value agrees with the absolute configuration expected from the synthetic route. Least-squares refinements were carried out by minimizing the function $\sum w(|F_o| - |F_c|)^2$, where F_o and F_c are the observed and calculated structure factors. The weighting scheme used in the last refinement cycles was $w = w'[1 - (\Delta F/6\sigma(F_o)^2]_2$ where $w' = 1/\sum_1^n A_r T_r(x)$ with three coefficients A_r for the Chebyshev polynomial $A_r T_r(x)$ where x was F_c/F_c(max).[18] Details of data collection and refinement are given in Table 1.

The calculations were carried out with the CRYSTALS package programs[19] running on a PC. The drawings of the molecules were produced with CAMERON.[20]

Calculation of the NLO Response. The all-valence INDO/S (intermediate neglect of differential overlap) method,[21] in connection

(16) Altomare, A.; Cascarano, G.; Giacovazzo, G.; Guagliardi, A.; Burla, M. C.; Polidori, G.; Camalli, M. SIR92—a program for automatic solution of crystal structures by direct methods. *J. Appl. Crystallogr.* **1994**, *27*, 435.
(17) Flack, H. *Acta Crystallogr*. **1983**, *A39*, 876.
(18) Prince, E. *Mathematical Techniques in Crystallography*; Springer-Verlag: Berlin, 1982.
(19) Watkin, D. J.; Prout, C. K.; Carruthers, J. R.; Betteridge, P. W. *CRYSTALS, Issue 10*; Chemical Crystallography Laboratory, University of Oxford: Oxford, U.K., 1996.
(20) Watkin, D. J.; Prout, C. K.; Pearce, L. J. *CAMERON*; Chemical Crystallography Laboratory, University of Oxford: Oxford, U.K., 1996.
(21) (a) Zerner, M.; Loew, G.; Kirchner, R; Mueller-Westerhoff, U. *J. Am. Chem. Soc.* **1980**, *102*, 589. (b) Anderson, W. P.; Edwards, D.; Zerner, M. C. *Inorg. Chem.* **1986**, *25*, 2728. (c) Bacon, A. D.; Zerner, M. C. *Theor. Chim. Acta* **1979**, *53*, 21. (d) Ridley, J.; Zerner, M. C. *Theor. Chim. Acta* **1973**, *32*, 111.

Table 1. Crystallographic Data for H_2L, NiL·EtOH, and MnLCl

	H_2L	NiL·EtOH	MnLCl
empirical formula	$C_{28}H_{40}N_4O_2$	$C_{28}H_{38}N_4O_2Ni·C_2H_5OH$	$C_{28}H_{38}N_4O_2ClMn$
fw	464.7	567.4	553.0
crystal system	monoclinic	monoclinic	orthorhombic
space group	*I*2	$P2_1$	$P2_12_12_1$
a, Å	15.487(2)	8.613(2)	7.233(2)
b, Å	8.1988(6)	21.714(4)	15.159(4)
c, Å	20.958(3)	15.870(4)	25.591(7)
β, deg	95.92(1)	91.02(2)	
V, Å^3	2647.0(5)	2967.6(8)	2806(1)
Z	4	4	4
T, °C	−93	20	20
λ, Å	0.710 73	0.710 73	0.710 73
ρ(calcd), g, cm^{-3}	1.166	1.270	1.309
μ(Mo Kα), cm^{-1}	0.692	6.897	5.771
$R(F_o)^a$	0.0438	0.0407	0.0462
$R_w(F_o)^a$	0.0490	0.0447	0.0558

[a] $R = \sum(||F_o| - |F_c||)/\sum(|F_o|)$ and $R_w = \sum w(|F_o| - |F_c|)^2/\sum w(F_o)^2]^{1/2}$.

with the sum-over excited-hole-states (SOS) formalism,[22] was employed. Details of the computationally efficient ZINDO−SOS-based method for describing second-order molecular optical nonlinearities have been reported elsewhere.[5,14,23] The monoexcited configuration interaction (MECI) approximation was employed to describe the excited states. In all calculations, the lowest 180 energy transitions between SCF and MECI electronic configurations were chosen to undergo CI mixing and were included in the SOS. Metrical parameters used for the calculations were taken from related crystal structure data (vide infra). The INDO/SCI−SOS method has been successfully used for the description of molecular linear and nonlinear optical responses of organic and organometallic compounds,[23] including bis(salicylaldiminato)metal(II) Schiff-base complexes.[14,15] The method is used here to calculate the second-order NLO response of H_2L and NiL on the basis of the crystal structures.

Nonlinear Optical Measurements. The measurements of second-harmonic generation (SHG) intensity were carried out by the Kurtz−Perry powder technique,[24,25] using a nanosecond Nd:YAG pulsed (10 Hz) laser operating at $\lambda = 1.064\ \mu$m. The additional 1.907 μm radiation was generated by the Raman effect: the fundamental beam (1.064 μm) was focused in a hydrogen cell (1 m long, 50 atm), and the outcoming Stokes-shifted radiation at 1.907 μm was used as the fundamental beam for second-harmonic generation. The SHG signal was detected by a photomultiplier and read on an ultrafast Tektronic 7834 oscilloscope. The samples, which were unsized microcrystalline powders obtained by grinding, were placed between two glass plates.

Results and Discussion

Synthesis and Characterization. Chiral Schiff-base complexes based on 1,2-diamines have been used in various catalytic asymmetric syntheses.[26] However, our first attempt to obtain the Schiff-base ligand by condensation of the diamine and salicylaldehyde in ethanol surprisingly failed and required a reaction in toluene with a Dean Stark apparatus. The experiment was monitored by ^{1}H NMR spectroscopy to verify the disappearance of the CHO signal located at 9.47 ppm in the starting (diethylamino)salicylaldehyde and the appearance of the imine signal at 7.92 ppm. Metal complexes were obtained by direct mixing of the appropriate metal salt with the diamine and aldehyde to take advantage of the chelating effect of the metal center. The oxidation of Mn(II) to Mn(III) during the synthetic process has been reported in the literature.[27−30] ^{1}H NMR spectra

Table 2. Atomic Coordinates and Equivalent Isotropic Displacement Parameters *U*(eq) for H_2L[a]

atom	*x*/*a*	*y*/*b*	*z*/*c*	*U*(eq), Å^2	*U*(iso), Å^2
		Molecule A			
O(1)	0.1939(1)	0.4824(2)	0.46583(8)	0.0451	
N(1)	0.0594(1)	0.6806(3)	0.4499(1)	0.0354	
C(11)	0.1626(2)	0.4102(3)	0.4102(1)	0.0326	
C(12)	0.0859(1)	0.4688(3)	0.3752(1)	0.0344	
C(13)	0.0569(2)	0.3833(4)	0.3194(1)	0.0450	
C(14)	0.1002(2)	0.2517(3)	0.2979(1)	0.0492	
C(15)	0.1780(2)	0.1959(3)	0.3326(1)	0.0420	
C(16)	0.2072(1)	0.2774(3)	0.3892(1)	0.0355	
C(121)	0.0381(2)	0.6050(3)	0.3973(1)	0.0363	
C(122)	0.0078(1)	0.8222(3)	0.4648(1)	0.0363	
C(123)	0.0544(2)	0.9777(4)	0.4471(1)	0.0488	
C(124)	0.0067(2)	1.1306(3)	0.4648(2)	0.0587	
N(15)	0.2239(2)	0.0691(3)	0.3094(1)	0.0571	
C(151)	0.1967(3)	−0.0131(7)	0.2492(2)	0.1027	
C(152)	0.1356(3)	−0.132(1)	0.2546(3)	0.1301	
C(153)	0.3037(2)	0.0083(4)	0.3433(1)	0.0525	
C(154)	0.2929(2)	−0.1123(4)	0.3961(2)	0.0603	
		Molecule **B**			
O(2)	−0.0119(1)	0.2977(3)	0.14697(9)	0.0466	
N(2)	−0.0552(1)	0.0892(3)	0.05322(9)	0.0319	
C(21)	−0.0932(1)	0.3600(3)	0.1349(1)	0.0311	
C(22)	−0.1526(1)	0.2929(3)	0.0872(1)	0.0304	
C(23)	−0.2338(1)	0.3665(3)	0.0772(1)	0.0358	
C(24)	−0.2572(1)	0.4979(3)	0.1120(1)	0.0380	
C(25)	−0.1979(2)	0.5651(3)	0.1608(1)	0.0353	
C(26)	−0.1154(2)	0.4942(3)	0.1708(1)	0.0374	
C(221)	−0.1300(1)	0.1582(3)	0.0476(1)	0.0305	
C(222)	−0.0445(1)	−0.0516(3)	0.0123(1)	0.0329	
C(223)	−0.0578(2)	−0.2076(4)	0.0505(1)	0.0465	
C(224)	−0.0449(2)	−0.3589(3)	0.0118(1)	0.0555	
N(25)	−0.2226(1)	0.6923(3)	0.1977(1)	0.0474	
C(251)	−0.3046(2)	0.7786(4)	0.1812(1)	0.0474	
C(252)	−0.3052(2)	0.8896(4)	0.1236(2)	0.0579	
C(253)	−0.1667(2)	0.7556(4)	0.2519(1)	0.0625	
C(254)	−0.1111(3)	0.8963(6)	0.2356(2)	0.0916	
H(1)	0.153(2)	0.569(4)	0.470(1)		0.059(6)
H(2)	−0.015(2)	0.220(4)	0.115(2)		0.059(6)

[a] Esd's in parentheses refer to the last significant digit. *U*(eq) is defined as the cube root of the product of the principal axes.

(22) Ward, J. F. *Rev. Mod. Phys.* **1965**, *37*, 1.
(23) (a) Kanis, D. R.; Ratner, M. A.; Marks, T. J. *J. Chem. Rev.* **1994**, *94*, 195. (b) Kanis, D. R.; Marks, T. J.; Ratner, M. A. *Int. J. Quantum Chem.* **1992**, *43*, 61.
(24) Kurtz, S. K.; Perry, T. T. *J. Appl. Phys.*, **1968**, *39*, 3798.
(25) Dougherty, J. P.; Kurtz, S. K. *J. Appl. Crystallogr.* **1976**, *9*, 145.
(26) (a) Palucki, M.; Pospisil, P. J.; Zhang, W.; Jacobsen, E. N. *J. Am. Chem. Soc.* **1994**, *116*, 9333. (b) Larrow, J. F.; Jacobsen, E. N. *J. Am. Chem. Soc.* **1994**, *116*, 12129. (c) Jacobsen, E. N.; Zhang, W.; Muci, A. R.; Ecker, J. R.; Deng, L. *J. Am. Chem. Soc.* **1991**, *113*, 7063.
(27) Bernardo, K.; Leppard, S.; Robert, A.; Commenges, G.; Dahan, F.; Meunier, B. *Inorg. Chem.* **1996**, *35*, 387.
(28) Oki, A. R.; Hodgson, D. J. *Inorg. Chim. Acta* **1990**, *170*, 65.
(29) Pecoraro, V. L.; Butler, W. M. *Acta Crystallogr.* **1986**, *C42*, 1151.

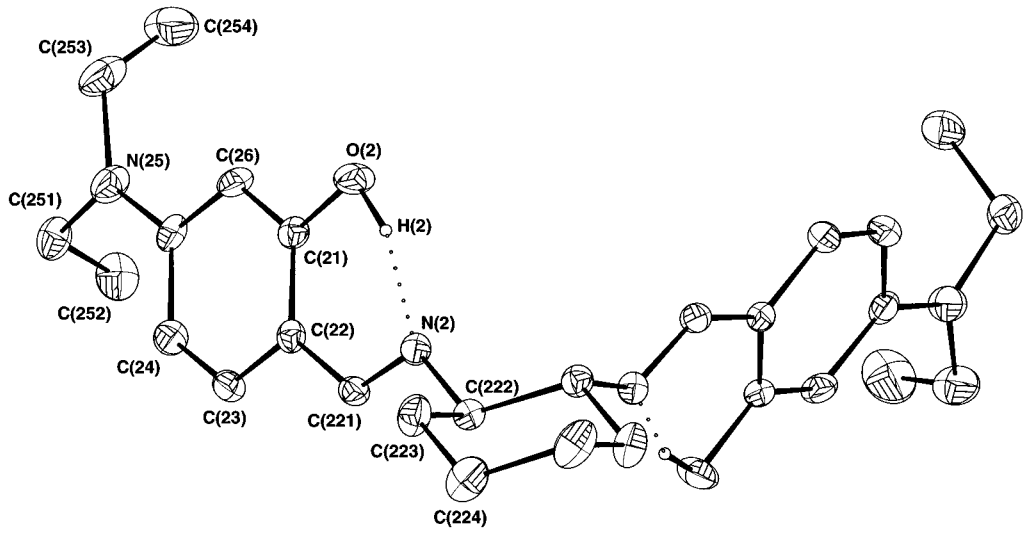

Figure 1. ORTEP view of H_2L.

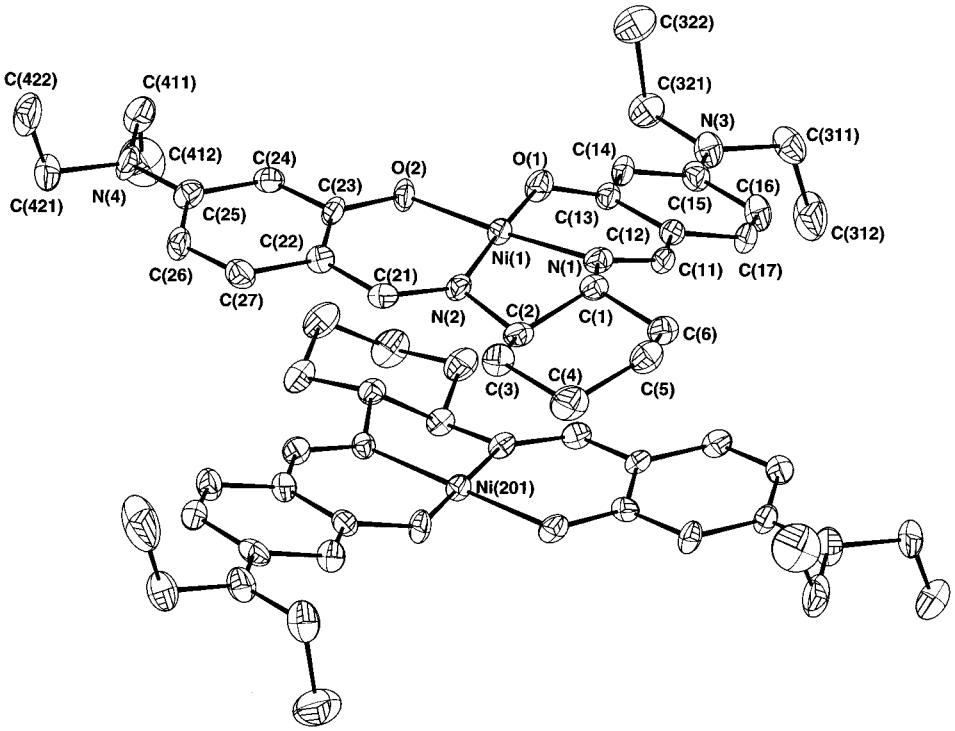

Figure 2. ORTEP view of NiL·EtOH. The two independent molecules of the unit cell are related by a pseudoinversion center.

are reported for H_2L and NiL·EtOH only, MnLCl being paramagnetic. Four hydrogen atoms of the cyclohexyl fragment could not be precisely located in the nickel derivative (multiplet around 1.20−1.40 ppm), because of the signal of a methyl group at 1.24 ppm. However, they have been detected by the integration signal and reported at 1.28 pm for a similar compound.[27]

Structural Studies. The molecular structure of H_2L and atom-labeling scheme are shown in Figure 1. The fractional atomic coordinates and equivalent isotropic thermal parameters are given in Table 2. The asymmetric unit contains two independent halves of the molecule which are arranged around different 2-fold axis. These two halves, **A** and **B**, are identical within experimental error. As observed in the related Schiff-base ligand $H_2NMe_2C_6Salen$,[27] the structure may be described as "open armed", the imine−aromatic ring moieties diverging outward from the cyclohexyl ring. Short O−H- - -N intramolecular hydrogen bonds (0.97(4), 1.73(3), and 0.92(4), 1.75(4) Å for **A** and **B**, respectively) indicate strong hydrogen bonding of the hydroxyl groups to the imine N.

The molecular structures of the Ni(II) and Mn(III) complexes and atom-labeling schemes are shown in Figures 2 and 3. Fractional atomic coordinates with equivalent isotropic or isotropic thermal parameters are given in Tables 3 and 4. Each asymmetric unit of the NiL·EtOH compound contains two independent molecules, **A** and **B**, related by a pseudoinversion center. These two molecules are arranged in a head to tail fashion, but there is no significant difference between their geometries. The nickel atoms lie in a nearly perfect square-planar coordination environment with deviations from the basal

(30) Davies, J. E.; Gatehouse, B. M.; Murray, K. S. *J. Chem. Soc., Dalton Trans.* **1973**, 2523.

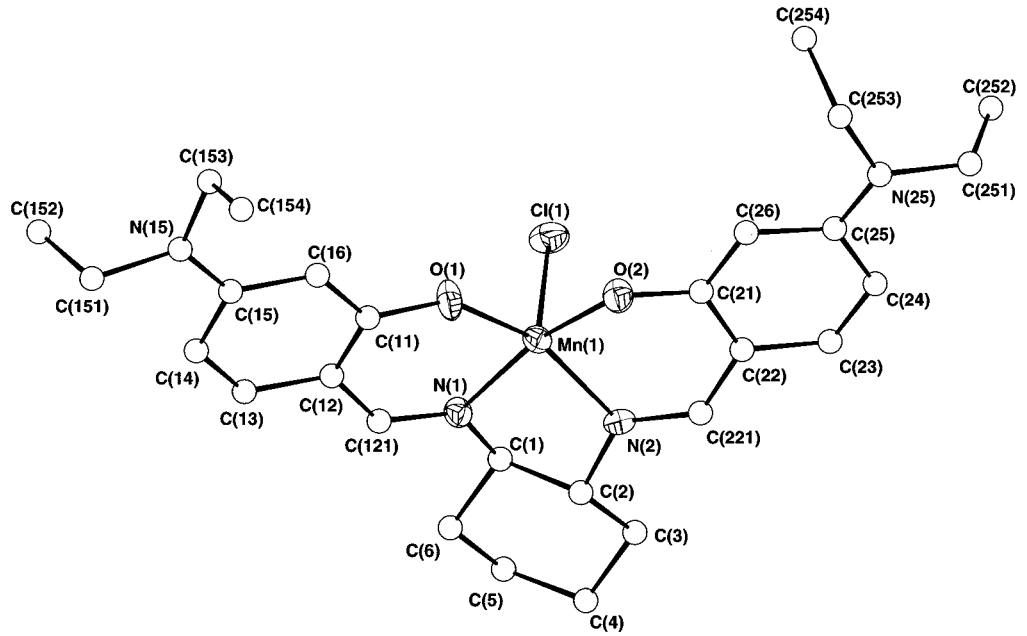

Figure 3. ORTEP view of MnLCl.

Table 3. Atomic Coordinates and Equivalent Isotropic Displacement Parameters *U*(eq) for NiL·EtOH

atom	*x*/*a*	*y*/*b*	*z*/*c*	*U*(eq), Å^2	atom	*x*/*a*	*y*/*b*	*z*/*c*	*U*(eq), Å^2
				Molecule **A**					
Ni(1)	0.06434(6)	0.62726(2)	0.33995(4)	0.0334	C(27)	0.2781(6)	0.8047(2)	0.2250(3)	0.0489
O(1)	0.0709(4)	0.5974(1)	0.4491(2)	0.0449	C(311)	0.0653(6)	0.3907(3)	0.7077(4)	0.0600
O(2)	0.1512(4)	0.6966(1)	0.3871(2)	0.0441	C(312)	0.1888(9)	0.3433(3)	0.7025(6)	0.0947
N(1)	−0.0379(4)	0.5588(2)	0.2955(2)	0.0403	C(321)	0.1719(6)	0.4963(3)	0.7298(4)	0.0597
N(2)	0.0820(4)	0.6531(2)	0.2304(2)	0.0379	C(322)	0.0497(8)	0.5370(3)	0.7670(4)	0.0780
N(3)	0.1088(5)	0.4510(2)	0.6686(3)	0.0504	C(411)	0.4180(7)	0.8819(3)	0.5043(4)	0.0699
N(4)	0.4105(5)	0.8882(2)	0.4129(3)	0.0502	C(412)	0.556(1)	0.8504(4)	0.5340(5)	0.1085
C(11)	−0.0547(5)	0.5068(2)	0.3344(3)	0.0424	C(421)	0.4692(7)	0.9452(3)	0.3770(4)	0.0625
C(12)	−0.0107(5)	0.4943(2)	0.4194(3)	0.0346	C(422)	0.3433(8)	0.9909(2)	0.3602(4)	0.0730
C(13)	0.0521(5)	0.5412(2)	0.4733(3)	0.0353	C(1)	−0.0929(4)	0.5693(2)	0.2080(3)	0.0359
C(14)	0.0904(6)	0.5245(2)	0.5542(3)	0.0436	C(2)	0.0357(5)	0.6055(2)	0.1670(3)	0.0400
C(15)	0.0705(5)	0.4658(2)	0.5882(3)	0.0435	C(3)	−0.0060(6)	0.6274(2)	0.0783(3)	0.0481
C(16)	0.0113(6)	0.4200(2)	0.5345(3)	0.0467	C(4)	−0.0562(7)	0.5714(3)	0.0273(4)	0.0658
C(17)	−0.0290(6)	0.4349(2)	0.4543(4)	0.0470	C(5)	−0.1842(6)	0.5337(2)	0.0684(3)	0.0538
C(21)	0.1454(5)	0.7046(2)	0.2043(3)	0.0351	C(6)	−0.1428(5)	0.5151(2)	0.1554(3)	0.0450
C(22)	0.2054(5)	0.7509(2)	0.2584(3)	0.0343	O(4)	0.8291(6)	0.1958(3)	0.4246(3)	0.1196
C(23)	0.2056(5)	0.7450(2)	0.3463(3)	0.0385	C(41)	0.984(2)	0.1945(5)	0.3917(8)	0.0805
C(24)	0.2761(5)	0.7905(2)	0.3973(3)	0.0418	C(42)	1.069(1)	0.2512(6)	0.420(1)	0.1463
C(25)	0.3476(6)	0.8446(2)	0.3637(3)	0.0449	C(43)	0.968(2)	0.2373(5)	0.4148(9)	0.1000
C(26)	0.3432(6)	0.8485(2)	0.2737(3)	0.0462	C(44)	1.097(1)	0.2000(8)	0.377(1)	0.1323
				Molecule **B**					
Ni(201)	0.42684(6)	0.57044(3)	0.16127(4)	0.0354	C(227)	0.2039(5)	0.3959(2)	0.2713(3)	0.0407
O(201)	0.4087(4)	0.6024(1)	0.0543(2)	0.0407	C(511)	0.4687(7)	0.8041(2)	−0.2093(4)	0.0617
O(202)	0.3482(4)	0.4996(1)	0.1116(2)	0.0414	C(512)	0.3432(9)	0.8517(4)	−0.2106(8)	0.1311
N(201)	0.5012(4)	0.6421(1)	0.2094(2)	0.0319	C(521)	0.3563(7)	0.7006(3)	−0.2295(4)	0.0615
N(202)	0.4345(4)	0.5367(1)	0.2697(2)	0.0319	C(522)	0.475(1)	0.6591(4)	−0.2687(6)	0.1163
N(203)	0.4198(5)	0.7460(2)	−0.1724(3)	0.0529	C(611)	0.0539(8)	0.3225(3)	−0.0076(4)	0.0782
N(204)	0.0569(6)	0.3164(2)	0.0837(3)	0.0604	C(612)	−0.068(1)	0.3661(4)	−0.0367(5)	0.1032
C(211)	0.5317(5)	0.6931(2)	0.1706(3)	0.0390	C(621)	−0.0040(7)	0.2581(3)	0.1157(4)	0.0673
C(212)	0.5093(5)	0.7037(2)	0.0853(3)	0.0425	C(622)	0.120(1)	0.2107(3)	0.1283(5)	0.0965
C(213)	0.4461(5)	0.6597(2)	0.0285(3)	0.0416	C(201)	0.5013(5)	0.6407(2)	0.3039(3)	0.0365
C(214)	0.4163(5)	0.6732(2)	−0.0580(3)	0.0399	C(202)	0.5276(5)	0.5747(2)	0.3281(3)	0.0395
C(215)	0.4488(5)	0.7330(2)	−0.0887(3)	0.0427	C(203)	0.5054(6)	0.5673(2)	0.4215(4)	0.0558
C(216)	0.5118(6)	0.7768(2)	−0.0292(3)	0.0528	C(204)	0.6128(7)	0.6099(3)	0.4714(3)	0.0629
C(217)	0.5380(6)	0.7626(2)	0.0514(3)	0.0468	C(205)	0.5891(7)	0.6752(3)	0.4454(4)	0.0615
C(221)	0.3629(5)	0.4872(2)	0.2915(3)	0.0408	C(206)	0.6074(6)	0.6848(2)	0.3504(4)	0.0527
C(222)	0.2801(5)	0.4469(2)	0.2359(3)	0.0360	O(5)	0.6743(6)	0.0085(3)	0.0743(4)	0.1255
C(223)	0.2789(5)	0.4531(2)	0.1481(3)	0.0329	C(51)	0.519(2)	−0.0023(9)	0.101(2)	0.1883
C(224)	0.2037(6)	0.4088(2)	0.0982(3)	0.0411	C(52)	0.467(1)	−0.0639(5)	0.070(1)	0.1091
C(225)	0.1318(5)	0.3596(2)	0.1340(3)	0.0417	C(53)	0.539(2)	−0.0303(8)	0.079(2)	0.1747
C(226)	0.1295(6)	0.3530(2)	0.2228(3)	0.0445	C(54)	0.413(1)	0.0049(7)	0.122(1)	0.1008

planes of 0.023 and 0.028 Å. Owing to the presence of the Cl atom, the Mn atom is 0.303 Å above the square basal plane and the geometry around the metal may be better regarded as a distorted square pyramid.

Table 4. Atomic Coordinates and Equivalent Isotropic Displacement Parameters *U*(eq) for MnLCl

atom	*x*/*a*	*y*/*b*	*z*/*c*	*U*(iso), Å^2	*U*(eq), Å^2
Mn(1)	0.0894(2)	0.56022(8)	0.17064(5)		0.0371
Cl(1)	0.2264(3)	0.6771(1)	0.2196(1)		0.0587
O(1)	0.2892(8)	0.5054(4)	0.1364(2)		0.0542
O(2)	0.0317(8)	0.6244(3)	0.1109(2)		0.0465
N(1)	0.099(1)	0.4727(4)	0.2276(2)		0.0385
N(2)	−0.1686(8)	0.5728(4)	0.1978(2)		0.0364
N(15)	0.795(1)	0.3165(6)	0.0965(4)	0.081(3)	
N(25)	−0.1918(9)	0.8704(4)	0.0161(2)	0.038(2)	
C(1)	−0.041(1)	0.4903(5)	0.2683(3)	0.041(2)	
C(2)	−0.218(1)	0.5098(5)	0.2398(3)	0.039(2)	
C(3)	−0.365(1)	0.5408(6)	0.2776(4)	0.058(3)	
C(4)	−0.393(2)	0.4719(6)	0.3193(4)	0.070(3)	
C(5)	−0.216(2)	0.4493(7)	0.3475(4)	0.072(3)	
C(6)	−0.068(1)	0.4204(5)	0.3101(3)	0.055(2)	
C(11)	0.390(1)	0.4356(5)	0.1490(3)	0.042(2)	
C(12)	0.356(1)	0.3864(6)	0.1947(4)	0.048(2)	
C(13)	0.470(1)	0.3116(6)	0.2045(4)	0.056(3)	
C(14)	0.610(1)	0.2897(6)	0.1727(4)	0.065(3)	
C(15)	0.649(1)	0.3388(6)	0.1275(4)	0.059(3)	
C(16)	0.537(1)	0.4128(5)	0.1168(4)	0.052(2)	
C(21)	−0.093(1)	0.6897(4)	0.1068(3)	0.035(2)	
C(22)	−0.248(1)	0.6933(5)	0.1407(3)	0.038(2)	
C(23)	−0.374(1)	0.7625(5)	0.1320(3)	0.043(2)	
C(24)	−0.355(1)	0.8222(5)	0.0927(3)	0.044(2)	
C(25)	−0.204(1)	0.8154(5)	0.0579(3)	0.036(2)	
C(26)	−0.071(1)	0.7492(5)	0.0668(3)	0.035(2)	
C(121)	0.210(1)	0.4065(5)	0.2301(4)	0.043(2)	
C(151)	0.889(2)	0.2287(8)	0.1023(5)	0.090(4)	
C(152)	1.045(3)	0.242(1)	0.1351(7)	0.145(7)	
C(153)	0.854(2)	0.3689(7)	0.0533(5)	0.083(4)	
C(154)	0.762(2)	0.344(1)	0.0037(6)	0.117(5)	
C(221)	−0.282(1)	0.6332(5)	0.1813(3)	0.041(2)	
C(251)	−0.319(1)	0.9447(7)	0.0087(3)	0.052(2)	
C(252)	−0.268(2)	1.0232(7)	0.0426(5)	0.077(3)	
C(253)	−0.038(1)	0.8645(5)	−0.0212(3)	0.047(2)	
C(254)	0.137(1)	0.9077(7)	−0.0031(4)	0.072(3)	

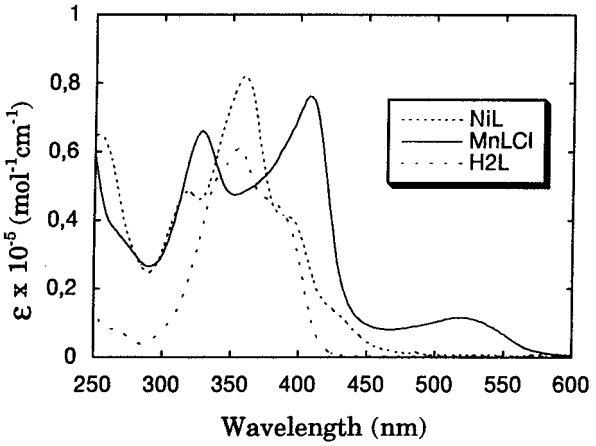

Figure 4. Optical spectra of H_2L, NiL, and MnL recorded in EtOH.

Optical Spectroscopy. The optical absorption spectra of the three materials are shown in Figure 4. Each spectrum exhibits an intense band at 354 nm (ϵ_{max} = 61 100 M^{-1} cm^{-1}), 358 nm (ϵ_{max} = 82 900 M^{-1} cm^{-1}), and 407 nm (ϵ_{max} = 76 400 M^{-1} cm^{-1}) for H_2L, NiL, and MnLCl, respectively, in ethanol solution. Additional, less intense bands are observed for each molecule at higher and lower energy. As previously reported,[14,15] a general trend is observed for a red shift upon metal complexation, this effect being more important in the case of the Mn(III) derivative with a low-lying optical transition located at 518 nm (ϵ_{max} = 12 100 M^{-1} cm^{-1}). Moreover, the above bands exhibit solvatochromic shifts (Table 5) characteristic of a large dipole moment change ($\Delta\mu$) between the ground and the excited state. In particular, a bathochromic (red) shift with increasing solvent polarity could be observed for the ligand ($\Delta\mu > 0$), while the complexes exhibited an opposite behavior. This solvatochromism appears to be more pronounced for the ligand than for the metal complexes.

INDO/SCI calculations provide a rationale for the above trend (Table 5). In the case of H_2L, the stronger band centered at 354 nm and the related shoulders at lower and higher energy can be related to a set of four calculated lowest-energy electronic transitions, the stronger of which having relevant charge transfer (CT) character ($\Delta\mu$ = 5.1 D), according with the observed solvatochromism. Analogously, for the NiL complex, a set of six transitions is predicted in the region between 264 and 419 nm, in good agreement with the optical spectrum and the observed red shift upon metal complexation (Figure 4). Moreover, these transitions possess CT character accompanied by a reduction of the dipole moment in the excited state ($\Delta\mu < 0$), in agreement with the observed solvatochromism.

Molecular Hyperpolarizabilities (β). The theoretical β_{xxx} (the largest hyperpolarizability tensor component) values of the H_2L and NiL are reported in Table 6. They indicate a sizable NLO response for this family of chromophores, comparable to that previously calculated and observed for salen derivatives.[14] As expected, on passing from the ligand to the Ni(II) complex, a relevant enhancement of β values is predicted, according with the calculated red shift of the low-lying CT optical transitions on passing from H_2L to NiL. The calculated negative sign of β for the Ni(II) complex indicates a reduction of the dipole moment ($\Delta\mu < 0$) between the ground and the excited states in the transitions responsible for the SHG response, while are predicted positive β values ($\Delta\mu > 0$) for the ligand.

Within the framework of the SOS perturbation theory, the molecular hyperpolarizability can be related to all excited states of the molecule and can be partitioned into two contributions, so-called two-level and three-level terms.[14a] Analysis of term contributions to the molecular hyperpolarizability of H_2L and NiL indicates that, in both cases, two-level terms dominate the nonlinearity. It can be related to a single low-lying electronic transition for the ligand, while many electronic states contribute to the nonlinearity of the Ni(II) complex. In particular, the 1 → 5 (HOMO → LUMO) based transition is essentially responsible for the nonlinearity of the ligand (Table 7). Turning to the Ni(II) derivative, the second-order nonlinearity can be mainly related to 1 → 4, 1 → 6, 1 → 8 electronic transitions. The 1 → 6 transition contributes about 40% to the nonlinearity and essentially involves the SHOMO and LUMO MO's. The difference in electronic population between the ground state and the dominant excited state discussed above for H_2L and NiL is shown in Figure 5. At first, the origin of the nonlinearity for these chiral compounds (**II**) seems to be very similar to that of the related derivatives (**I**) containing the CN withdrawing substituents.[15] Both diethylamino groups and nickel atoms act as electron donors, while the imine groups are the acceptor counterpart of the molecules. It can be noticed that the 1,2-carbon atoms of the cyclohexane ring in **II** do not play any role in the charge-transfer process. This is in agreement with the general trend observed for the simple ethylene and phenylene bridge derivatives,[14] but in contrast with **I**, in which the whole "N═C−C═C−C═N" linkage is involved in the nonlinearity.[15]

Nonlinear Susceptibility ($\chi^{(2)}$). The bulk efficiencies recorded on powder samples for the three materials are gathered in Table 8 versus that of a powder sample of urea recorded as a reference. The more limited accuracy of the measurements

Table 5. Absorption Maxima of the Lowest Energy Optical Transitions for H_2L, NiL, and MnLCl in Solvents of Different Polarities and INDO/SCI Lowest Energy Derived Values

	λ^{expt}_{max}, nm							λ^{calc}_{max}, nm	f^{calc}
	methanol	ethanol	MeCN	EtOAc	THF	chloroform	CCl_4		
	340 (sh)	340 (sh)						295	0.71
								302	0.19
H_2L	356	354	330	322	324	336	326	311	0.19
								317	0.33
	378 (sh)	376 (sh)	376 (sh)	338 (sh)	342 (sh)	370 (sh)	342 (sh)		
								264	0.14
	317	316	319	320	321	322	324	313	0.36
								328	0.55
NiL	358	358	358	361	362	366	370	365	0.44
								372	0.18
	389	392	392	400	402	397	408	419	0.17
	326	327	327	328	328	331			
MnLCl	406	407	410	413	415	418	insoluble		
	517	518	517	519	520	526			

Table 6. INDO/SCI−SOS Second-Order NLO Responses (10^{-30} cm^5 esu^{-1}) for H_2L and NiL at Various Wavelengths (Incident Laser Beam)

	λ, μm	β_{xxx}		λ, μm	β_{xxx}
H_2L	0.0	7.3	NiL	0.0	−9.0
	1.907	8.5		1.907	−10.5
	1.064	12.4		1.064	−16.2

at 1.907 μm versus those at 1.064 μm is explained by the lowest power supplied by the laser at this wavelength and by the poor signal-to-noise ratio of the photomultiplier provided in the infrared (0.954 μm). On the other hand, the significant absorption observed at the double frequency (0.532 μm) for the manganese derivative (Figure 4) can readily account for the surprisingly low efficiency recorded at 1.064 μm. Therefore the value at 1.907 μm is the only one to be taken into account for this derivative. The ligand and Ni(II) complex being transparent at 532 nm can be compared with a suitable accuracy at 1.064 μm.

When the powder efficiencies are tentatively related to the molecular hyperpolarizability (β), it appears that, although the INDO/SCI−SOS calculations predict an enhancement of the nonlinearity after metal complexation, the Ni(II) derivative exhibits a very modest efficiency compared to the ligand. This can be readily understood by careful examination of the crystal structure. It is well-known that chirality provides the synthetic chemist with a means of guaranteeing that crystallization of a pure enantiomer will occur in a noncentrosymmetric point group. However, the fact that a molecule is optically pure does not guarantee that the molecular packing will be optimized for NLO effects. For instance, the charge-transfer pathways in successive molecules may oppose each other, thus canceling the major part of β, whereas the cyclohexyl groups, which do not contribute significantly to the nonlinearity, may form an oriented sublattice. This type of unexpected structure was observed in the Ni(II) derivative. An angle of 178.3° can be measured between the charge-transfer axis of two neighboring molecules, indicating an almost centrosymmetric structure (Figure 2). This pseudo-centrosymmetry can account for the very low efficiency recorded for this compound. Although it seems natural to attach a quantitative meaning to chirality, it is meaningless to refer to our derivatives as being "weakly chiral", as this concept is not quantified.[31] However, it is clear that Schiff-base molecules made from (1*R*,2*R*)-(−)-1,2-diaminocyclohexane or (1*S*,2*S*)-(+)-1,2-diaminocyclohexane would be similar and hence the asymmetry of these molecules is only slight. Other diamines chosen to enhance the asymmetry are currently under investigation.

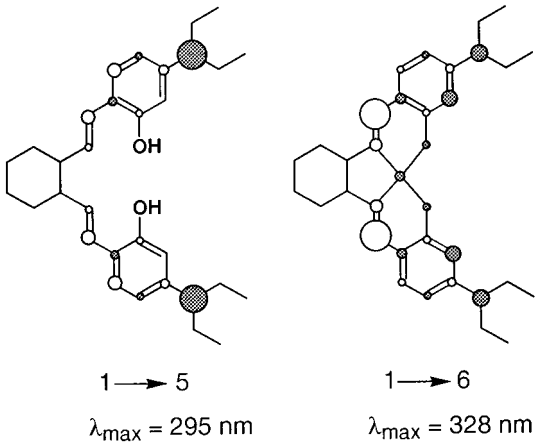

Figure 5. Difference in electronic populations between the ground state and the excited state for the main transitions involved in the NLO response of H_2L (left) and NiL (right). The black contribution is indicative of a decrease in electron density in the charge-transfer process.

The higher powder efficiency observed in the manganese derivative cannot be understood as precisely. Since this compound is paramagnetic (4.957 $\mu_B \approx 4$ unpaired electrons), no hyperpolarizability theoretical calculations can be performed; thus no data are currently available concerning its molecular hyperpolarizability. However, a qualitative comparison between NiL and MnLCl can be proposed on the basis of optical spectra (Figure 4) and solvatochromism (Table 5). Compared to the case of the Ni(II) complex, the observed stronger CT absorptions and the existence of the additional low-lying CT feature both suggest that this compound may exhibit a molecular hyperpolarizability higher than that of the Ni(II) derivative.[14a]

Relations between microscopic and macroscopic optical nonlinearities are strongly dependent on the orientation of β with respect to the crystalline reference frame and the nature of the relevant point group. The crystal structure of MnLCl is $P2_12_12_1$ (point group 222), for which the only nonvanishing component of $\chi^{(2)}$ is[32]

$$d_{XYZ} = (4/V)(f^{2\omega}{}_X)(f^{\omega}{}_Y)(f^{\omega}{}_Z)(\sin\phi)(\cos\phi)(\cos\theta)(\sin^2\theta)\cdot\beta_{xxx}$$

where V is the volume cell, f_X, f_Y, and f_Z are Lorentz local-field factors, and ϕ and θ are angular parameters defined from the

(31) Buda, A. B.; Auf der Heyde, T.; Mislow, K. *Angew. Chem., Int. Ed. Engl.* **1992**, *31*, 989.

(32) Zyss, J.; Oudar, J. L. *Phys. Rev. A* **1982**, *26*, 2028.

Table 7. Energy (λ_{max}, nm), Oscillator Strength (f), Dipole Moment Change between Ground and Excited States ($\Delta\mu$, D), and Composition of the Dominant Excited State Involved in the Nonlinearity for H_2L and NiL

	trans	λ_{max}	f	$\Delta\mu$	composition[a] of CI expansion
H_2L	$1 \rightarrow 5$	295	0.71	5.1	$0.52_{\chi 91\rightarrow 94} - 0.21_{\chi 91\rightarrow 95} + 0.21_{\chi 91\rightarrow 96} - 0.56_{\chi 92\rightarrow 93} - 0.21_{\chi 92\rightarrow 95} - 0.22_{\chi 92\rightarrow 96}$
NiL	$1 \rightarrow 6$	328	0.55	−5.9	$-0.30_{\chi 93\rightarrow 97} + 0.27_{\chi 93\rightarrow 98} - 0.41_{\chi 94\rightarrow 97} - 0.35_{\chi 94\rightarrow 98} + 0.57_{\chi 95\rightarrow 97} + 0.25_{\chi 95\rightarrow 98}$

[a] Orbital 92 is the HOMO and orbital 93 the LUMO for H_2L. Orbital 96 is the HOMO and orbital 97 the LUMO for NiL.

Table 8. Powder SHG Efficiencies (Referred to Urea) for H_2L, NiL·EtOH, and MnLCl

	at 1.064 μm	at 1.907 μm
H_2L	0.25	< 0.25 (limit of detection)
NiL·EtOH	0.1	< 0.25 (limit of detection)
MnLCl	0.5 (absorption)	8

Euler spherical angle.[32] The optimal value of the angular factor is 0.192, reached for $\theta = 55°$ and $\phi = 45°$. Assuming a one-dimensional β_{xxx} along the charge-transfer axis of the MnLCl molecule, we found $\theta = 104°$ and $\phi = 122°$, which gives an angular factor of 0.089 versus 0.110 calculated for 3-methy-4-nitropyridine 1-oxide (POM), a molecular material that crystallizes in space group $P2_12_12_1$ and was proposed for electrooptic applications.[33,34]

Conclusion

This paper described the synthesis and characterization of new optically active Schiff-base complexes. Evidence was provided (INDO/SCI−SOS calculations and solvatochromism) for a sizable NLO response and for an enhancement of the nonlinearity after metal complexation. The chirality of the ligand is a useful strategy for engineering the chromophores into acentric crystal structures. This approach has been successfully used for the Mn(III) derivative, while the relatively low powder efficiency of the Ni(II) derivative has been related to the quasicentrosymmetric packing structure. Further studies based on other chiral ligands are currently in progress.

Acknowledgment. We thank the Centre National de la Recherche Scientifique (CNRS, Paris) and the Consiglio Nazionale delle Ricerche (CNR, Rome) for financial support.

Supporting Information Available: Listings of X-ray experimental details, full interatomic distances, bond angles, anisotropic thermal parameters for non-hydrogen atoms, and atomic coordinates for hydrogen atoms (13 pages). Ordering information is given on any current masthead page.

IC970481W

(33) Zyss, J.; Chemla, D. S.; Nicoud, J. F. *J. Chem. Phys.* **1981**, *74*, 4800.
(34) Sigelle, M.; Hierle, R. *J. Appl. Phys.* **1981**, *52*, 4199.